Inference of weak nuclear collectivity from atomic masses

J. N. Orce[1,*]

[1] *TRIUMF, 4004 Wesbrook Mall, Vancouver, BC V6T 2A3, Canada*

(Dated: July 26, 2010)

We explore weakly-collective singly-closed shell nuclei with high-j shells where active valence neutrons and particle-particle correlations may be the dominant collective degree of freedom. The combination of large and close-lying proton and neutron pairing gaps extracted from experimental masses seems to charaterize the origin of the weak collectivity observed in Ni and Sn superfluids with $N \approx Z$. The trend of $E2$ transition strengths, i.e., $B(E2; 2_1^+ \rightarrow 0_1^+)$ values, in these nuclei is predicted from proton and neutron pairing-gap information. The agreement with the Ni isotopes is excellent and recent experimental results support the trend in the Sn isotopes. This work emphasizes the importance of atomic masses in elucidating nuclear-structure properties. In particular, it indicates that many-body microscopic properties such as nuclear collectivity could be directly inferred from more macroscopic average properties such as atomic masses.

PACS numbers: 21.10.Re, 21.60.Cs, 21.60.Ev, 23.20.-g, 27.60.+j

Nuclear collectivity is controlled by the interplay of particle-hole (ph) and particle-particle (pp) excitations. Particle-hole correlations produce deformation through the proton-neutron (pn) interaction and give rise to nuclear rotations [1]. In this work, we search for weakly-collective low-lying structures in $N \approx Z$ nuclei where pp correlations may, a priori, be the dominant degree of freedom. Large separation energies between single-particle orbits due to the spin-orbit interaction [3], together with the attractive short-range pairing interaction acting on $J = 0$ Cooper pairs [4] should lead to specially stable and spherical nuclei. Singly-closed shell Ni ($Z = 28$) and Sn ($Z = 50$) isotopes with $N \gtrsim 28$ and $N \gtrsim 50$ are characterized by weakly-collective reduced transition probabilities, i.e., $B(E2; 2_1^+ \rightarrow 0_1^+)$ values. Moreover, small quadrupole moments of $Q_S(2_1^+) \approx 0.05$ eb have been determined for $^{60-62}$Ni and ^{112}Sn from reorientation-effect measurements [5]. Quadrupole collectivity cannot solely arise from valence neutrons and proton-core excitations are needed to account for such weakly-collective systems. Proton-core excitations are supported by the positive g *factors* of 2_1^+ states in the even-mass $^{58-64}$Ni isotopes [6] and the enhancement of $B(E2; 2_1^+ \rightarrow 0_1^+)$ values observed in the neutron-deficient Sn isotopes as the $N = 50$ shell closure is approached [7–12].

The latter unveils one of the major conflicts encountered by the nuclear shell model (SM). Plainly, large-scale SM calculations predict an inverse parabolic trend of $B(E2; 2_1^+ \rightarrow 0_1^+)$ values peaking at midshell and cannot reproduce the enhancement of $E2$ strengths determined in the $^{106-112}$Sn isotopes using ^{88}Sr, ^{90}Zr or ^{100}Sn cores [7, 8]. The former cores provide better results and support proton-core excitations. A similarly baffling scenario has recently been revealed by Jungclaus and collaborators at midshell of the tin isotopic chain [13]. High-statistics Coulomb-excitation measurements in inverse kinematics and fits to lineshapes have provided very accurate lifetimes for the 2_1^+ states in the ^{112,114,116}Sn isotopes. Longer lifetimes from the accepted values in the nuclear data evaluation [14] yield $B(E2; 2_1^+ \rightarrow 0_1^+)$ values which clearly deviate from the inverse parabolic trend at midshell and, instead, propose a conspicuous minimum at ^{116}Sn; in agreement with $N = 66$ being a subshell closure.

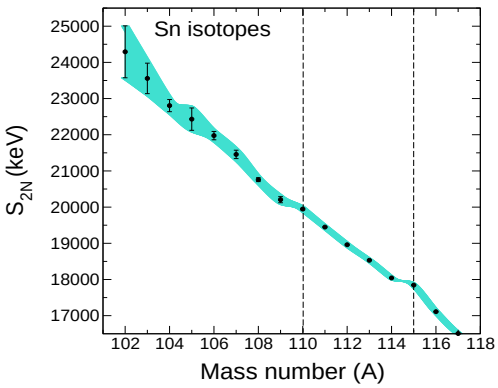

FIG. 1. (Color online) Two-neutron separation energies for the $^{102-117}$Sn isotopes. Small deviations from the smooth trend arise at ^{110}Sn and ^{115}Sn. A cubic-spline interpolation has been used for visual purposes.

Furthermore, average nuclear properties such as charge radii and quadrupole deformations are directly related, through a density function, to ground-state masses [15–18]. Similarly, nuclear masses provide a sensitive indicator, through binding energies, for structural changes within an isotopic chain. A beautiful example is given by the high-precision mass measurements of neutron-rich Mo, Zr and Sr isotopes [19], where a major change in nuclear structure is deduced from the smooth trend in two-neutron separation energies, S_{2N}. An onset of defor-

* jnorce@triumf.ca; http://www.pa.uky.edu/~jnorce

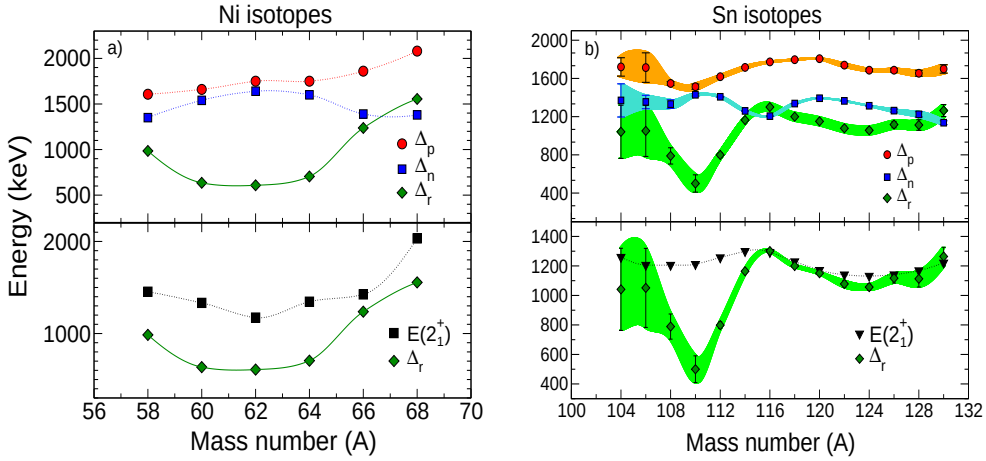

FIG. 2. (Color online) The top panel shows proton, Δ_p, neutron, Δ_n and relative Δ_r, pairing gaps extracted from the 2003 Atomic Mass Evaluation (AME03) [25] for the even-mass Ni (left) and Sn (right) isotopes. The bottom panel shows a comparison of 2_1^+ excitation energies and Δ_r values. A cubic-spline interpolation has been used to remark uncertainty effects of Δ_r values in the Sn isotopes. Mass uncertainties regarding pairing gaps in the Ni isotopes are considered negligible, although this is not the case for ^{68}Ni.

mation at $N = 60$ for ^{100}Zr and ^{98}Sr, as compared with much weaker deformations in more neutron-deficient isotopes, is characterized by a sudden drop in the binding energies. Shape coexistence has been observed and strong rotational bands built on the ground state and low-lying 0_2^+ excitations in ^{100}Zr and ^{98}Sr [14]. Further high-precision mass measurements of neutron-rich Sn isotopes advocates for a restoration of the $N = 82$ shell closure [20, 21]. Figure 1 shows S_{2N} values from ^{102}Sn to ^{117}Sn. Small deviations from the smooth trend at ^{110}Sn and ^{115}Sn may suggest structural changes. The latter points at the $N = 66$ subshell gap as supported by the minimum in the collective trend at ^{116}Sn [13]. The origin of the small deviation at ^{110}Sn is more obscure. This work attempts at elucidating whether weakly-collective $B(E2; 2_1^+ \rightarrow 0_1^+)$ values in the Ni and Sn isotopes and atomic masses are related in a comprehensive manner.

Within the BCS pairing model [4] the 2_1^+ excitation is created by breaking one Cooper pair, and is interpreted as a two quasiparticle which lies at least twice the pairing energy, 2Δ. For $N \approx Z$ nuclei, proton and neutron Fermi surfaces lie close to each other, henceforth we assume that the interplay of both proton and neutron pairing gaps may contribute to the overall oscillation of the Fermi surface and the collective origin of the 2_1^+ state [22–24]. Intuitively, we introduce the *relative pairing gap*, Δ_r, defined by,

$$\Delta_r^2 \equiv \mid (\Delta_p - \Delta_n)(\Delta_p + \Delta_n) \mid = \mid \Delta_p^2 - \Delta_n^2 \mid, \quad (1)$$

where the first term $(\Delta_p - \Delta_n)$ is the *r*esonant factor, which accounts for the proximity of proton and neutron pairing-gaps. That is, the smaller the energy difference between both pairing gaps, the larger the overlap of proton and neutron pairing fields. The second term $(\Delta_p + \Delta_n)$ is the *e*nergy factor, and accounts for the energy that can be provided to the nuclear system before breaking Cooper pairs, i.e., a quantity that enhances the possibility of having spherical nuclei, where vibrations may occur.

The magnitude of the neutron, Δ_n, and proton, Δ_p, pairing gaps can be determined from experimental odd-even mass differences [25] derived from the Taylor expansion of the nuclear mass in nucleon-number differences [15]. These prescriptions assume that pairing is the only non-smooth contribution to nuclear masses. We extract Δ_n and Δ_p from the symmetric five-point difference [15], which accounts better for blocking effects in odd-mass nuclei between shell gaps [27],

$$\Delta_n^{(5)} = -\frac{1}{8}[M(Z,N+2) - 4M(Z,N+1) + 6M(Z,N) - 4M(Z,N-1) + M(Z,N-2)] \quad (2)$$

$$\Delta_p^{(5)} = -\frac{1}{8}[M(Z+2,N) - 4M(Z+1,N) + 6M(Z,N) - 4M(Z-1,N) + M(Z-2,N)]. \quad (3)$$

Here, we make the strong assumption of a valid Δ_p in the region of study, although the kink of binding energies at shell closures would, a priori, not allow a Taylor expansion. This assumption is supported by the ^{56}Ni and ^{100}Sn soft cores and Ref. [27]. Doubly magic ^{56}Ni and ^{100}Sn are not included in the pairing-gap systematics since in these cases both magic-number and Wigner cusps span singularities in the mass surface [28]. The top panel of Fig. 2 shows Δ_n and Δ_p in the even-mass Ni (left panel) and Sn (right panel) isotopes. As expected, Δ_n lies lower than the corresponding Δ_p.

For comparison, Δ_r values and 2_1^+ excitation energies in the $^{58-68}$Ni and $^{104-130}$Sn isotopes are plotted in the

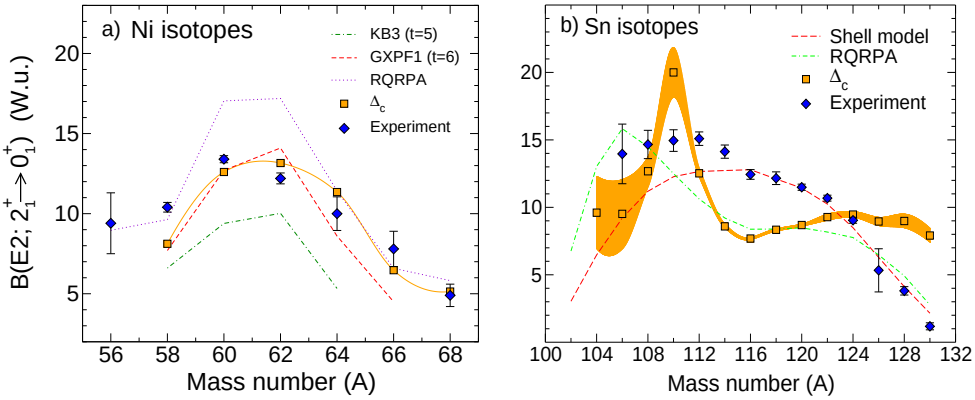

FIG. 3. (Color online) Experimental $B(E2; 2_1^+ \rightarrow 0_1^+)$ weighted averages [6–12, 26, 30] and Δ_c values in even-mass a) Ni and b) Sn isotopes. Δ_c values are given in units of MeV^{-1}. Available MF (RQRPA) [34] and large-scale SM [7, 33] calculations are shown for comparison. The quantity t refers to the number of nucleons that are excited from the $f_{7/2}$ orbit to the remaining fp shell using either the KB3 or GXPF1 effective interactions. A cubic-spline interpolation has been used to remark uncertainty effects of Δ_r values in the Sn isotopes. Mass uncertainties regarding pairing gaps in the Ni isotopes are considered negligible.

bottom panels of Fig. 2 (left and right panels, respectively). Excitation energies and Δ_r values follow a similar trend at $^{60-64}$Ni and differ for ^{58}Ni and $^{66-68}$Ni. For instance, whereas the energy difference of the 2_1^+ states in ^{58}Ni and ^{66}Ni is only $\sim$ 30 keV, there is a sharper energy difference of 150 keV between their Δ_r values. $\Delta_r = 0.985$ MeV for ^{58}Ni and it decreases to minimum values of $\Delta_r = 0.635$ and 0.608 MeV for ^{60}Ni and for ^{62}Ni, respectively. Protons and neutron pairing gaps begin to diverge at ^{64}Ni, $\Delta_r = 0.705$ MeV, with Δ_n becoming much smaller than Δ_p. $\Delta_r = 1.237$ MeV in ^{66}Ni, and has a maximum value of $\Delta_r = 1.555$ MeV at ^{68}Ni, where Δ_p has a maximum energy of $\sim$2.1 MeV and $\Delta_p - \Delta_n$ has the largest energy difference.

Moreover, Δ_r values and 2_1^+ energies in the Sn isotopes follow a similar parabolic trend from ^{116}Sn to ^{130}Sn. However, unlike excitation energies, the trend of Δ_r values between ^{104}Sn to ^{116}Sn clearly shows a sharp minimum at ^{110}Sn with $\Delta_r = 0.498$ MeV. For lighter and heavier Sn isotopes, proton and neutron pairing gaps begin to diverge, with Δ_r values of 0.791 and 0.799 MeV at ^{108}Sn and ^{112}Sn, respectively. Δ_r increases to a maximum value of 1.300 MeV for ^{116}Sn. From ^{116}Sn to ^{130}Sn, Δ_r values follow a smooth parabolic trend, with Δ_r being larger than for $^{108-112}$Sn. Larger Δ_r values of 1.076 and 1.010 MeV are found for ^{104}Sn and ^{106}Sn, respectively. A strong correlation with quadrupole collectivity can be inferred from the trends of Δ_r values in the Ni and Sn isotopes.

From a global fit to available $B(E2; 0_1^+ \rightarrow 2_1^+)$ values throughout the nuclear chart, Grodzins deduced an exceptional formula that calculates surprisingly well $B(E2; 0_1^+ \rightarrow 2_1^+)$ values from well-known 2_1^+ energies [29]. Raman improved the fit from a larger data set [30] and the Grodzins-Raman's empirical formula is given by,

$$B(E2; 0_1^+ \rightarrow 2_1^+) = (2.57 \pm 0.45)\, Z^2 A^{-2/3} E(2_1^+)^{-1} \quad (4)$$

The physical meaning of this formula remains unknown. Similarly, given the qualitative agreement between Δ_r values and 2_1^+ energies in the even-mass Ni and Sn isotopes, $E2$ collectivity might be estimated using the inverse of Δ_r. For that, the *pairing-gap collective strength*, Δ_c, is defined as,

$$\Delta_c \equiv \frac{2\Omega}{\Delta_r}, \quad (5)$$

where $2\Omega = (2j+1)$ is the average particle number, i.e., the total number of proton and neutron Cooper pairs that may contribute to the collective motion. Δ_c values are given in units of $[E^{-1}]$. In order to examine the interplay of proton-core excitations and pp correlations for Ni and Sn isotopes with $N \approx Z$, only the $f_{7/2}$ and $g_{9/2}$ proton and neutron orbits, respectively, will be included in Eq. 5. These orbits are fully occupied and the large spacial overlap of magnetic substates may enhance pairing correlations. This assumption may not be valid for the very neutron-rich Sn isotopes.

The origin of Eq. 5 lies within the BCS framework. For the special case of a pure pairing force in a single-j shell, the gap equation yields the two-quasiparticle energy [31, 32],

$$E_k + E_{k'} = 2\Delta = G\,\Omega, \quad (6)$$

where $E_k, E_{k'}$ are the quasiparticle energies at the Fermi surface and G the pairing strength. Given the qualitative agreement between Δ_r and 2_1^+ energies, it can be assumed that $2\Delta \approx \Delta_r$ and Eq. 5 can be written as,

$$\Delta_c \approx \frac{2}{G}. \quad (7)$$

That is, nuclear collectivity is inversely proportional to the pairing strength.

Finally, Fig. 3 shows the systematics of experimental $B(E2; 2_1^+ \rightarrow 0_1^+)$ values (blue diamonds) as compared with single-particle estimates (1 W.u.) in the even-mass $^{58-68}$Ni [6, 26, 30] and $^{106-130}$Sn isotopes [7, 8, 12]. Strikingly, the trend of $E2$ strengths in these Ni isotopes is in agreement with Δ_c values (left panel of Fig. 3). In fact, the trend of Δ_c values provides a better agreement than large-scale SM [33] and MF [34] calculations. For ^{62}Ni, Δ_c presents a maximum in the systematics which corresponds to the lowest 2_1^+ energy and the strongest collectivity predicted by large-scale SM [33] and MF [34] calculations.

The trend of quadrupole collectivity in the Sn isotopes is not as precisely defined as in the Ni isotopes, although the enhancement of collectivity in the neutron-deficient Sn isotopes is well established. The trend of Δ_c values in the Sn isotopes is plotted in the right panel of Fig. 3 and shows an enhancement of $E2$ strengths in the neutron-deficient Sn isotopes, with a sharp maximum at ^{110}Sn. MF calculations also indicate a sharp maximum in the trend of $E2$ strengths [34], but peaking at ^{106}Sn. This maximum is unlikely since the energy spectrum of ^{106}Sn shows typical properties of singly closed-shell nuclei that can simply be explained with a δ-function interaction. The $B(E2; 2_1^+ \rightarrow 0_1^+)$ values for ^{104}Sn and ^{106}Sn are, respectively, either unknown or with large uncertainties. The most precise $B(E2; 2_1^+ \rightarrow 0_1^+)$ in ^{106}Sn by Ekström and collaborators indicates, however, a decreasing trend with a smaller $B(E2; 2_1^+ \rightarrow 0_1^+) = 13.1(2.6)$ W.u. as compared with ^{108}Sn [9], in agreement with the trend proposed in this work. In addition, Jungclaus and coworkers have recently determined much lower and precise $E2$ strengths for ^{112,114,116}Sn, with decreasing absolute $B(E2; 2_1^+ \rightarrow 0_1^+)$ values from ^{112}Sn to ^{116}Sn (not plotted in this work). These remarkable results point at ^{116}Sn as the new minimum in the collective trend at midshell, in disagreement with large-scale SM calculations, and supporting the $N = 66$ subshell closure and the current work. Summarizing, this work proposes that microscopic many-body properties such as nuclear collectivity could be inferred from atomic masses.

Further transition strengths and mass measurements are needed in the neutron-deficient and mid-shell Sn region to confirm the collective trend proposed in this work. In particular, more accurate experimental data is needed in the key ^{110}Sn isotope. Curiously, the experimental masses accepted in the 2003 atomic mass evaluation concerning pairing gaps in ^{110}Sn are either from unpublished private communications or based on β end-point measurements [25].

The author gratefully acknowledges fruitful discussions with U. Hesse-Orce, S. Baroni, M. Brodeur, M. Honma, A. Ansari, C. J. Lister, B. Singh and S. W. Yates. TRIUMF receives federal funding via a contribution agreement through the National Research Council of Canada.

[1] J.L. Wood, K. Heyde, W. Nazarewicz, M. Huyse, and P. Van Duppen, Phys. Rep. **215**, 101 (1992).
[2] P. E. Garrett and J. L. Wood, J. Phys. G **37**, 069701 (2010).
[3] M. G. Mayer and J. H. D. Jensen, *E*lementary Theory of Nuclear Shell Structure (Wiley, New York, 1955).
[4] L. Cooper, J. Bardeen, and J. Schrieffer, Phys. Rev. **108**, 1175 (1957).
[5] N. J. Stone, At. Data Nucl. Data Tables **90**, 75 (2005).
[6] O. Kenn, K.-H. Speidel, R. Ernst, J. Gerber, N. Benczer-Koller, G. Kumbartzki, P. Maier-Komor, F. Nowacki, Phys. Rev. C**63**, 021302(R) (2000).
[7] A. Banu *et al.,* Phys. Rev. C **72**, 061305(R) (2005).
[8] J. Cederkäll, *et al.,* Phys. Rev. Lett. **98**, 172501 (2007).
[9] A. Ekström *et al.,* Phys. Rev. Lett. 101, 012502 (2008).
[10] J. N. Orce *et al.,* Phys. Rev. C **77**, 029902(E) (2008).
[11] R. Kumar *et al.*, Phys. Rev. C **81**, 024306 (2010).
[12] C. Vaman *et al.,* Phys. Rev. Lett. **99**, 162501 (2007).
[13] A. Jungclaus *et al.,* presented at the INPC 2010 conference and accepted for publication in Phys. Lett. B (2010).
[14] http://www.nndc.bnl.gov. (*NNDC database*)
[15] P. Möller, J. R. Nix, W. D. Myers and W. J. Swiatecki, Atomic Data Nucl. Data Tables **59**, 185 (1995).
[16] W. D. Myers and W. J. Swiatecki, Nucl. Phys. A**601**, 141 (1996).
[17] S. Goriely, F. Tondeur and J.M. Pearson, Atomic Data Nucl. Data Tables **77**, 311 (2001).
[18] S. Goriely, M. Samyn and J.M. Pearson, Phys. Rev. C **75**, 064312 (2007).
[19] U. Hager *et al.*, Phys. Rev. Lett. **96**, 042504 (2006).
[20] M. Dworschak *et al.*, Phys. Rev. Lett. **100**, 072501 (2008).
[21] K. L. Jones *et al.*, Nature, **465**, 454 (2010).
[22] A. Bohr, Compt. Rend. Congres Int. de Physique Nucleaire, Paris, Vol. I, 487 (1964).
[23] D.R. Bes, R.A. Broglia, O. Hansen, and O. Nathan, Phys. Rep. **34**, 1 (1977).
[24] R.A. Broglia, O. Hansen, and C. Riedel, Adv. Nucl. Phys. **6**, 287 (1973).
[25] G. Audi, A.H. Wapstra and C. Thibault. Nucl. Phys. A**729**, 337 (2003).
[26] J. N. Orce *et al.,* Phys. Rev. C **77**, 064301 (2008).
[27] M. Bender, K. Rutz, P. -G. Reinhard, J. A. Maruhn, Eur. Phys. J. A **8**, 59 (2000).
[28] D.G. Madland, and J.R. Nix, Nucl. Phys. **A476**, 1 (1988).
[29] L. Grodzins, Phys. Lett. **2**, 88 (1962).
[30] S. Raman, C.W. Nestor Jr., P. Tikkanen, At. Data Nucl. Data Tables **78**, 1 (2001).
[31] P. Ring and P. Schuck, *The Nuclear Many-Body Problem, Springer (2004).*
[32] Jouni Suhonen, *From Nucleons to Nucleus. Concepts of Microscopic Nuclear Theory, Springer (2007).*
[33] M. Honma, T. Otsuka, B.A. Brown, T. Mizusaki, Phys. Rev. C **69**, 034335 (2004).
[34] A. Ansari, and P. Ring, Phys. Rev. C **74**, 054313 (2006).